Characterization of the CCL21-mediated melanoma-specific immune responses and *in situ* melanoma eradication

Laura Novak, Olga Igoucheva, Stephanie Cho, and Vitali Alexeev

Department of Dermatology and Cutaneous Biology, Jefferson Medical College, Thomas Jefferson University, Philadelphia, Pennsylvania

Abstract

Previous studies have shown that secondary lymphoid chemokine, CCL21, can be used for modulation of tumor-specific immune responses. Here, using B16F0 melanoma cells stably expressing CCL21 under the control of cytomegalovirus and ubiquitin promoters, we showed that CCL21-activated immune responses depend on the amount of melanoma-derived chemokine, which, in turn, depends on the strength of the promoter. We showed that ubiquitin promoter–driven expression of CCL21 enabled massive infiltration of tumors with $CD4^+CD25^-$, $CD8^+$ T lymphocytes, and $CD11c^+$ dendritic cells, and consequent activation of cellular and humoral immune responses sufficient for complete rejection of CCL21-positive melanomas within 3 weeks in all tumor-inoculated mice. Mice that rejected CCL21-positive tumors acquired protective immunity against melanoma, which was transferable to naive mice via splenocytes and central memory T cells. Moreover, melanoma-derived CCL21 facilitated immune-mediated remission of preestablished, distant wild-type melanomas. Overall, these results suggest that elevated levels of tumor-derived CCL21 are required for the activation of strong melanoma-specific immune responses and generation of protective immunologic memory. They also open new perspectives for the development of novel vaccination strategies against melanoma, which use intratumoral delivery of the optimized CCL21-encoding vectors in conjunction with DNA-based vaccines. [Mol Cancer Ther 2007;6(6):1755–64]

Introduction

The incidence of cutaneous malignant melanoma is increasing at a faster rate than any other cancer, both globally and in the United States (1). Immunotherapy has emerged as one of the most promising treatments of this melanocytic malignancy. Various vaccine therapies to achieve immune-based melanoma rejection have been successfully tested in preclinical animal models and several clinical trials. However, clinical studies have shown that existing therapeutic approaches are generally ineffective or prohibitively expensive.

Recently, chemokines have attracted considerable interest within the field of tumor immunotherapy. Chemokines are small proteins that are involved in immune and inflammatory responses. One of them, secondary lymphoid chemokine CCL21 (also known as SLC or C6kine), is prominently expressed in high endothelial venules and within T-cell zones of secondary lymphoid organs, where it recruits naive T cells and antigen-presenting cell (APC), such as dendritic cell, via a mechanism known as chemoattraction. This mechanism is based on CCL21-mediated activation of the G protein–coupled receptor CCR7, which is expressed in maturing dendritic cell and T lymphocytes. Interaction between the ligand (CCL21) and the receptor (CCR7) triggers a cascade of intracellular events that promotes changes in expression of adhesion molecules and cytoskeletal rearrangement. These changes enable directional migration of the $CCR7^+$ cells along the CCL21 gradient (2).

It has thus been suggested that this chemokine may promote recruitment of APC and T lymphocytes to a tumor mass to facilitate antigen recognition and enhance tumor-specific immune responses. In support of this concept, it was recently shown that the presence of CCL21 in the vicinity of a tumor induces infiltration of tumors with dendritic cell and $CD8^+$ T cell and leads to immune-mediated inhibition of melanoma (3), lung (4), and colon (5) carcinomas in experimental animals. Splenocytes isolated from these CCL21-treated mice showed greatly enhanced CTL activity against tumor cells (5). The chemoattractive properties of CCL21 were also used in the development of the dendritic cell–based vaccines. Using adenoviral gene transfer, CCL21 was expressed in tumor-associated antigen–pulsed dendritic cell. Treatment of tumor-bearing mice with these genetically altered dendritic cells resulted in tumor growth inhibition and remission in some of the experimental tumors (3, 6). However, in these various experimental tumor models, the utilization of CCL21 as a protein, even at a very high dosage or in combination with dendritic cell–based and DNA-based vaccines (5–8), resulted in temporal remission of tumors or in their complete obliteration in 20% to 60% of experimental animals.

Received 11/15/06; revised 4/9/07; accepted 5/1/07.

Grant support: Jefferson Medical College (V. Alexeev) and American Skin Association medical student grant (L. Novak).

The costs of publication of this article were defrayed in part by the payment of page charges. This article must therefore be hereby marked *advertisement* in accordance with 18 U.S.C. Section 1734 solely to indicate this fact.

Requests for reprints: Vitali Alexeev, Department of Dermatology and Cutaneous Biology, Jefferson Medical College, Thomas Jefferson University, 233 South 10th Street, BLSB, Room 326, Philadelphia, PA 19107. Phone: 215-503-4835; Fax: 215-503-5788. E-mail: vitali.alexeev@jefferson.edu

doi:10.1158/1535-7163.MCT-06-0709

Our current data show that strong ubiquitin promoter–driven expression of CCL21 led to elevated levels of melanoma-derived CCL21, which stimulated massive infiltration of both $CD4^+$ and $CD8^+$ T cells into developing melanomas, activation of melanoma-specific immune responses, and generation of strong, melanoma-specific protective immunity that was transferable into naive mice via splenocytes and $CD8^+$ central memory T cells (T_{CM}). CCL21-induced immune responses were sufficient for the obliteration of primary CCL21-positive tumors as well as obliteration of wild-type (WT) B16F0 melanomas inoculated at distant sites. In contrast to previous findings, these responses were observed in all animals inoculated with CCL21-expressing melanomas.

Materials and Methods

Cloning of Murine CCL21

Murine CCL21 cDNA (Genbank accession no. MMU88322) was amplified from total RNA extracted from mouse lymph nodes via reverse transcription-PCR using 5′-ATGGCTCAGATGATGACTCTGAGCCTC-3′ direct and 5′-ATGGAGAGCAGGTTCAGGTCT-3′ reverse primers. The PCR product was subcloned into pCUB and pcNDA 3.1 Zeo expression vectors under the control of ubiquitin and cytomegalovirus (CMV) promoters, respectively. Plasmids were designated as pCUB-CCL21 and pCMV-CCL21.

Cell Culture

B16F0 mouse melanoma cells were obtained from the American Type Culture Collection (CRL6332). Derivative CCL21-positive B16F0 cells were cultured in DMEM supplemented with 10% fetal bovine serum, 2 mmol/L L-glutamine, and 10 mg/mL penicillin/streptomycin. Medium and supplements were purchased from Invitrogen. Normal mouse melanocytes, Melan-a, were kindly provided by Dr. D. Bennett (St. George's Medical School, London, United Kingdom).

Generation of the CCL21-Expressing Melanoma Cells

CCL21-expressing B16F0 melanoma cells were generated via cotransfection of parental B16F0 cells with pPur (Invitrogen) and either pCUB-CCL21 or pCMV-CCL21 vectors followed by selection with puromycin (1 μg/mL) for 4 weeks. Puromycin-selected single clones were analyzed for CCL21 expression and secretion. Individual clones showing the highest levels of CMV-driven and ubiquitin promoter–driven expression of CCL21 were established as cell lines and designated as B16F0-CMV-CCL21 and B16F0-UB-CCL21, respectively. In parallel, mock-transfected and selected clones were established and designated as B16F0-CMV-Mock and B16F0-UB-Mock, respectively.

Western Blotting and ELISA Assays

For CCL21 expression and secretion analysis by Western blot, B16F0 and CCL21-expressing B16F0 cells were grown to 80% confluency and then either lysed or cultured for an additional 72 h in a serum-free medium. The serum-free medium was collected and concentrated 50 times. Proteins from lysates and concentrated medium were separated on 18% Tris-glycine gels, transferred onto polyvinylidene difluoride membranes, and probed with CCL21-specific antibodies (R&D Systems) diluted 1:5,000. Immunocomplexes were detected by horseradish peroxidase–labeled secondary antibodies and visualized using SuperSignal WestFemto Detection kit (Pierce). For the quantitative ELISA assay, B16F0, B16F0-CMV-CCL21, and B16F0-UB-CCL21 cells from pools and individual clones were seeded in 100 μL of culture medium onto 96-well plates (5×10^5 per well) and kept in culture for 48 h. Medium was then collected, purified, and subjected to the mouse CCL21 ELISA assay (R&D Systems) as advised by the manufacturer.

In vivo Tumor Inoculation and Monitoring

CCL21-mediated activation of melanoma-specific immune responses was tested *in vivo* on naive C57BL6 (Charles River Laboratories) and B6.CB17-Prkdc^{scid}/SzJ [C57BL6 background severe combined immunodeficient (SCID); The Jackson Laboratory] mouse strains. Three groups of naive (nine animals per group) and three groups of SCID (nine animals per group) mice were inoculated with B16F0, B16F0-CMV-CCL21, or B16F0-UB-CCL21 melanoma. Two additional groups of C57BL6 mice were inoculated with B16F0-CMV-Mock and B16F0-UB-Mock cells. Tumors were inoculated via i.d. injection of 1×10^5 cells per animal into the right flank. Developing tumors were monitored and measured with Vernier calipers twice weekly for 3 weeks unless otherwise stated. Tumor growth for each animal was recorded as tumor area. At the end of the first, second, and third weeks, control (B16F0 inoculated) and experimental (B16F0-CMV-CCL21 and B16F-UB-CCL21 inoculated) animals ($n = 3$ per group per each time point) were euthanized and tumors were excised, measured, and either snap frozen for indirect immunofluorescence or used for other assays as described below. For the prolonged experiments and collection of splenocytes and blood sera, an additional four groups of naive C57BL6 mice (five animals per group) were inoculated with B16F0-UB-CCL21 cells as described above.

Indirect Immunofluorescence

Tumor samples collected at various time points were embedded into OCT compound (Sakura Finetek USA, Inc.) and frozen. Sections (7 μm) were fixed with methanol for 13 min at −20°C, washed with TBS, blocked with 1% bovine serum albumin in TBS for 1 h, and incubated with primary antibodies overnight at +4°C. Immunocomplexes were detected with secondary antibodies labeled with Alexa Fluor^{488} or Alexa Fluor^{594} (Invitrogen). Antibodies against mouse CD45, CD4, CD8, and CD25 were from R&D Systems. Antibodies against CD11c were from BD PharMingen.

Preparation of Splenocytes, Lymphocytes, $CD8^+$ T cells, and Fluorescence-Activated Cell Sorting Analysis

Splenocytes were isolated from excised spleens according to standard protocol (9). For the analysis of tumor-infiltrating lymphocytes, excised tumors were minced into small pieces, and single-cell suspensions were obtained in

a similar way as the splenocytes. An enriched population of $CD8^+$ T cells was obtained by negative selection using MACS superparamagnetic microbeads (Miltenyi Biotech) according to the manufacturer's protocols and used for the assessment of cytotoxicity.

For the fluorescence-activated cell sorting (FACS) analysis, equal aliquots of single-cell suspensions (1×10^5 cells per assay) from spleens or tumors were incubated with anti-CD4, anti-CD8 antibodies conjugated with FITC, or anti-CD45 antibodies conjugated with phycoerythrin (R&D Systems) according to the manufacturer's protocols. Quantitation of labeled cells was done by FACS using CellQuest software (BD Bioscience).

Annexin-Based and Live/Dead Cytotoxicity Assays

The cytotoxicity of the lymphoid cells isolated from naive, B16F0-inoculated, and B16F0-UB-CCL21–inoculated mice was measured against B16F0, B16F0-UB-CCL21, Melan-a, and CHO-K1 target cells by Annexin-based cytotoxicity assay described previously (10). Briefly, splenocytes were cultured *in vitro* for 5 days in the presence of the complete medium or B16F0 cell extracts. Duplicate aliquots of effector cells (1×10^6) were mixed with target cells (2×10^4; E:T = 50) and incubated for 2 h. Corresponding target cells incubated in complete medium only were used as controls for spontaneous cell death. Cells were then washed in PBS and resuspended in Annexin-binding buffer containing Annexin-FITC (Roche Bioscience). Following incubation for 25 min, cells were washed and resuspended in 0.5 mL PBS and subjected to FACS analysis. The percentage of cytotoxicity was determined by the formula $(D - C) / (T - C) \times 100$, where D is the number of Annexin-positive target cells ($FITC^+$) incubated with lymphocytes, C is number of $FITC^+$ cell incubated in medium only, and T is the total number of target cells counted.

The cytotoxicity of splenocytes and enriched $CD8^+$ T cells was also measured using flow cytometry–based live/dead cell–mediated cytotoxicity assay (Invitrogen). Before the assay, all splenocytes were depleted from macrophages by the adherence method, and all effector cells were cultured in the presence of B16F0 cell extracts as described above. Effector cells were incubated with $DiOC_{18}$-labeled target cells (B16F0 or YAC-1, 1×10^4 per reaction) for 4 h at 37°C in different E:T ratios. Damaged cells were labeled with propidium iodide for 30 min at 37°C and analyzed by FACS. A two-variable cytogram was plotted. DiO^+PI^- and DiO^+PI^+ signals in lower-right and upper-right quadrant were counted for live target and dead target cells, respectively. Cytotoxicity was determined by the following formula: $[(DiO^+PI^+ / DiO^+PI^-)_{+\ \text{effectors}} - (DiO^+PI^+ / DiO^+PI^-)_{-\ \text{effectors}}] \times 100\%$.

Analysis of Humoral Immune Responses

To determine the presence of the melanoma-reactive antibodies, blood samples were collected from all animals at the time of euthanasia. Sera were obtained according to standard protocol (11) and analyzed for the presence of melanoma/melanocyte-reactive antibodies by a whole-cell immunofluorescence assay. B16F0 and Melan-a cells (1×10^4 per well) were seeded onto 96-well plates and cultured for 24 h. Cells were fixed with −20°C cold methanol and blocked with 1% bovine serum albumin in TBS. Diluted mouse serum (50 μL; 1:20 or 1:200) from control and experimental mice was added to the wells and incubated at +4°C overnight. Melanoma/melanocyte-bound antibodies were detected by Alexa $Fluor^{488}$–conjugated anti-mouse Ig (Invitrogen). Fluorescence intensity was measured on the Biotech FL600 fluorescence plate reader (Biotech, Inc.).

Challenge and Adoptive Transfer

Two weeks after complete rejection of the B16F0-UB-CCL21 tumors, mice ($n = 6$) were challenged with i.d. inoculation of WT B16F0 cells (1×10^5 per inoculation) into the left flanks. Tumor development was monitored thrice weekly.

To show adoptive transfer, mice that rejected CCL21-positive and secondary B16F0 tumors were additionally challenged with B16F0 tumors 40 days after rejection of the second challenge. Concurrently, naive C57BL6 mice (three groups, five animals per group) were inoculated with 5×10^5 B16F0 cells. Seven days after tumor inoculation, splenocytes were isolated from the challenged mice ($n = 2$) and from the B16F0-inoculated naive mice (control splenocytes). Splenic cells were transferred into another set of B16F0-inoculated naive mice via i.v. injection, one group in this set ($n = 5$) receiving control splenocytes and another group receiving cells isolated from tumor-rejecting animals. Immune-mediated rejection of WT melanomas was monitored as described above.

For the isolation of the $CD8^+$ T_{CM} cells, $CD8^+CD62L^{high}$ T cells were selected from the total population of splenocytes isolated from tumor-rejecting mice by negative selection using MACS superparamagnetic microbeads. $CD8^+CD62L^{high}$ cells were labeled with FITC-conjugated anti-CD44 antibodies and life sorted on the Coulter EPICS Elite cell sorter (BD Bioscience). The resultant population of the $CD8^+CD62L^{high}CD44^{high}$ was designated as T_{CM} cells. These cells were i.v. injected into a third group of B16F0-inoculated naive mice. Immune-mediated rejection of WT melanomas in these mice was monitored as described above.

CCL21-Mediated Rejection of Distal Melanoma

Two groups of mice ($n = 5$ per group) were inoculated in the right and left flanks with 1×10^5 WT B16F0 and B16F0-UB-CCL21 cells, respectively. Two additional control groups of animals ($n = 5$) were inoculated in a similar way with B16F0 and B16F0-UB-Mock cells. Tumor development in these mice was monitored for 3 weeks twice weekly as described above.

Statistical Analysis

For comparisons of individual groups, one-way ANOVA tests were done. For comparisons of two treatment groups, Student's t tests were done. Statistical significance is achieved at $P < 0.05$.

Results

Characterization of the CCL21-Expressing Melanoma Cells

Single individual clones of B16F0 cells stably expressing murine CCL21 under the control of CMV and ubiquitin promoters (B16F0-CMV-CCL21 and B16F0-UB-CCL21) were selected according to the expression of the chemokine (Fig. 1A). The levels of the CCL21 expression and secretion in established cell lines were determined by Western blot and ELISA analyses. As shown on Fig. 1B, ubiquitin-driven secretion of CCL21 into culture medium was approximately four times greater than that driven by the CMV promoter as determined by densitometric analysis of the Western blots. ELISA-based quantitation of CCL21 secretion showed that, during 48 h, 5×10^5 B16F0-UB-CCL21 cells secreted 5.4 times more chemokine (820 pg) than B16F0-CMV-CCL21 cells (150 pg; Fig. 1C).

Tumor Rejection Mediated by Melanoma-Derived CCL21

To investigate whether melanoma-derived CCL21 triggers attraction of immune cells and immune-mediated eradication of tumors *in vivo*, B16F0, control (B16F0-CMV-Mock and B16F0-UB-Mock), B16F0-CMV-CCL21, and B16F0-UB-CCL21 cells were i.d. injected into C57BL6 and SCID mice. During the first week of tumor development, the differences between control and experimental tumors were insignificant in both mouse strains (Fig. 2A). However, within 11 days, WT and control melanomas increased in size, whereas CCL21-expressing tumors did not grow beyond 12 mm^2 in C57BL6 mice. After this time point, WT and control tumors progressed rapidly, whereas B16F0-CMV-CCL21 tumors remained at approximately the same size for at least an additional 4 days. In contrast, B16F0-UB-CCL21 melanomas started to regress and shrank on average to 6 mm^2 by day 15 in all animals. At later time points, B16F0-CMV-CCL21 tumors restarted their growth, whereas B16F0-UB-CCL21 melanomas gradually regressed. Based on size and weight measurements at 2 weeks after tumor inoculation (Fig. 2B), WT melanomas were on average five times bigger than B16F0-UB-CCL21 tumors. By day 21, animals bearing WT and control melanomas were euthanized, B16F0-CMV-CCL21 melanomas progressed, whereas B16F0-UB-CCL21 tumors were barely detected in mouse skin as pigmented spots (Fig. 2B). By day 40, no visible tumors were present in mice inoculated with B16F0-UB-CCL21 cells.

When B16F0 and B16F0-UB-CCL21 cells were injected into SCID mice, no significant difference in growth rates between control and CCL21-expressing tumors was observed, indicating the important role of adaptive immunity in the rejection of CCL21-positive melanomas.

CCL21-Mediated Recruitment of APCs, T Lymphocytes, and Cytotoxic Immune Responses

To investigate the mechanism of CCL21-mediated tumor rejection, we analyzed the phenotypes of infiltrating cells in tumors excised 2 weeks after inoculation by indirect immunofluorescence. Initially, we examined the presence of the $CD11c^+$ APC and $CD45^+$ leukocytes in WT and B16F0-UB-CCL21 tumors. As compared with B16F0 melanomas, CCL21-positive tumors were characterized by the increased presence of $CD11c^+$ APC and a massive infiltrate of $CD45^+$ cells in deeper recesses of the tumor mass. Interestingly, $CD45^+$ cells evenly infiltrated the tumors, whereas $CD11c^+$ cells were primarily detected at the periphery (Fig. 3A). Most of the $CD45^+$-infiltrating cells expressed CD4, whereas the majority of leukocytes on the periphery expressed CD8. The majority of tumor-infiltrating $CD4^+$ T cells were $CD25^-$, although some of the cells at the periphery were identified as $CD4^+CD25^+$ regulatory T cells (Fig. 3A).

To verify the data obtained by indirect immunofluorescence, we did quantitative FACS analysis. As shown in Fig. 3B, during the first week of tumor development, both $CD4^+$

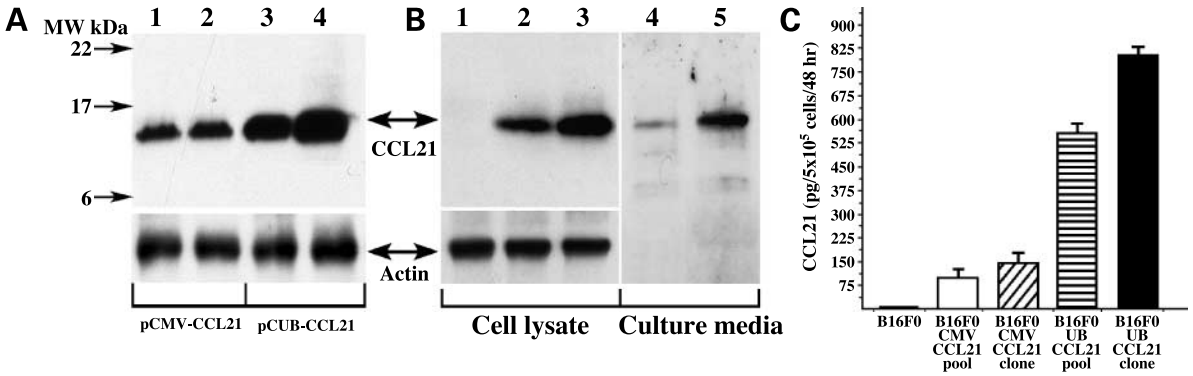

Figure 1. CCL21 expression and secretion in B16F0 melanoma cells. **A,** CCL21 expression in pCMV-CCL21–transfected and pCUB-CCL21–transfected Melan-a mouse melanocytes (*lanes 1* and *3*) and B16F0 mouse melanoma cells (*lanes 2* and *4*). **B,** expression and secretion of CCL21 in established CCL21-positive B16F0 cell lines. *Lane 1,* B16F0; *lane 2,* B16F0-CMV-CCL21; *lane 3,* B16F0-UB-CCL21; *lane 4,* culture medium from B16F0-CMV-CCL21; *lane 5,* culture medium from B16F0-UB-CCL21. *Arrows on the left,* point to apparent molecular weight (kDa). *Arrows between the panels,* point to CCL21 and actin (loading control). **C,** ELISA-based quantitation of CCL21 secretion in pooled and clonal B16F0 cells. *Bottom,* cell types. The assay was done in triplicates. *Columns,* mean of three independent experiments; *bars,* SD.

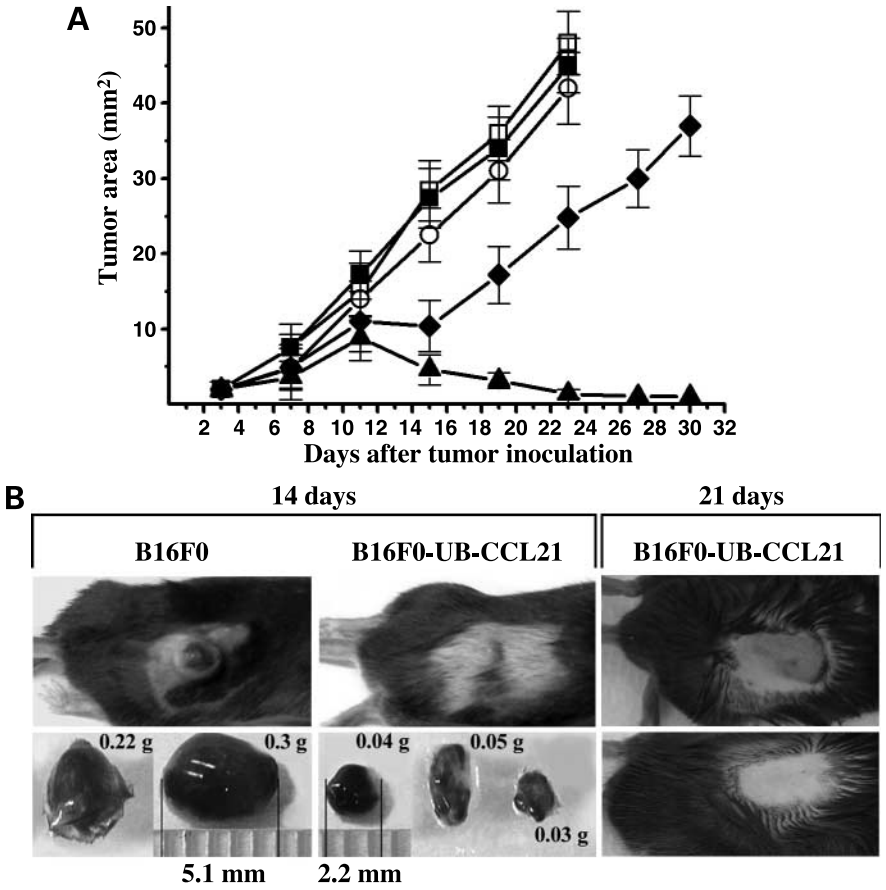

Figure 2. Development of the WT and CCL21-positive tumors. **A,** development of the WT and CCL21-positive tumors in C57BL6 and B6.CB17-Prkdc^{scid}/SzJ mice. Area of the tumors was calculated by multiplication of the length of the longest axis to the shortest. *Points,* mean; *bars,* SD. □ and ■, B16F0 and B16F0-UB-Mock tumors in C57BL6 mice, respectively; ○, B16F0-UB-CCL21 tumors in SCID mice; ♦, B16F0-CMV-CCL21 tumors in C57BL6 mice; ▲, B16F0-UB-CCL21 tumors in C57BL6 mice. **B,** photographs of the representative WT and CCL21-positive melanomas developed in C57BL6 mice 14 and 21 d after tumor inoculation. *Top,* tumor type. Tumor size and weight shown on the photographs of the excised tumors.

and CD8$^+$ T cells were actively recruited to the CCL21-expressing melanomas. However, at 2 weeks, 35% of total cells infiltrating the tumors were CD45$^+$ leukocytes, of which 60% were CD4$^+$ and 35% were CD8$^+$ T lymphocytes.

Melanoma-specific cytotoxicity of splenocytes was assessed by the Annexin V–binding CTL assay. As shown in Fig. 3C, splenocytes isolated from tumor-rejecting mice exhibit cytotoxicity toward all melanocytic cells (Melan-a, B16F0, and B16F0-CCL21). However, these cells were twice as effective in killing WT and CCL21-positive melanoma compared with melanocytes (Melan-a). The cytotoxicity of splenocytes toward melanoma cells was on average 3.4 times greater than that of the splenocytes from B16F0-inoculated animals and 7.5 times greater than that of splenocytes isolated from naive mice. We further determined the contribution of different cell types to the overall lytic effect using B16F0 and YAC-1 cells as targets, the total population of splenic cells, and CD8$^+$ T cells as effectors. As shown on Fig. 3D, at an E:T ratio of 50, 8% of total splenic cell cytotoxicity was found to be natural killer cell dependent, whereas 45% was found to be CD8$^+$ T lymphocyte dependent, as seen from the lytic activity of splenic cells against YAC-1 and B16F0 targets.

Humoral Immune Responses

To investigate whether CCL21-mediated infiltration of tumors with CD4$^+$ T cells leads to the activation of humoral immunity, sera collected from B16F0-inoculated and B16F0-UB-CCL21–inoculated mice sacrificed 2 weeks after tumor inoculation were examined for the presence of the melanoma/melanocyte-reactive antibodies. As determined by whole-cell immunofluorescence assays, sera from all B16F0-UB-CCL21–inoculated animals contained antibodies that recognized melanoma-derived antigens. Based on fluorescence intensity, serum samples (1:20 dilution) showed an average of 42% cross-reactivity with melanoma when compared with a positive control (gp100-specific αPEP13 antibodies; Fig. 4A and B). At a higher dilution of both sera and αPEP13 antibodies (1:200), serum samples showed 54% cross-reactivity of the positive control. In contrast, only one serum sample from B16F0-inoculated animals (mouse 2) showed low reactivity with melanoma cells. Sera from all B16F0-UB-CCL21–inoculated animals were also found to be cross-reactive with mouse melanocytes (Melan-a), suggesting recognition of shared antigens (Fig. 4C and D).

Challenge, Adoptive Transfer, and Rejection of Distal Melanoma

To investigate whether mice that rejected primary CCL21-positive tumors acquired protective immunity against WT melanoma, tumor-rejecting mice (n = 5) were inoculated with secondary B16F0 tumors 20 days after complete remission of primary tumors (Fig. 5A). Although

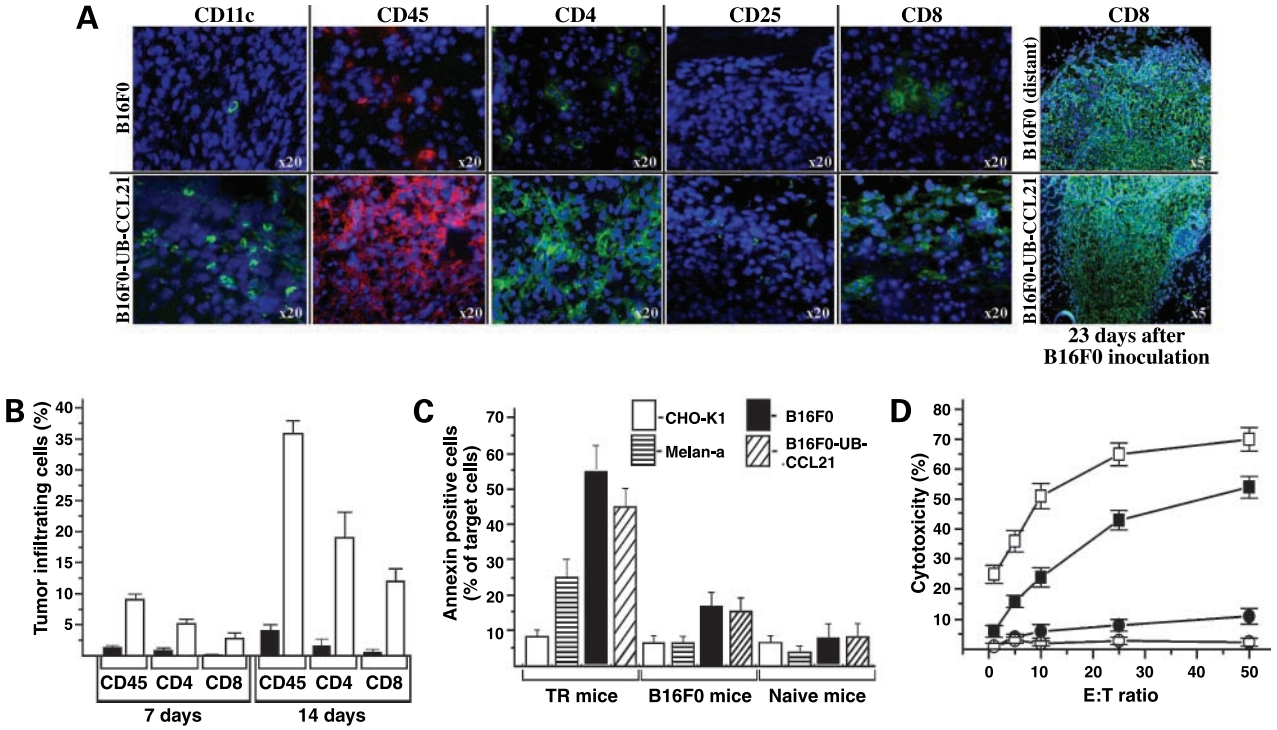

Figure 3. Tumor infiltration and cytotoxic immune response. **A,** photographs of representative cryosections of tumors stained with antibodies specific to immune cell markers as indicated above the photographs (*green* or *red*). *Blue,* cell nuclei were stained with 4′,6-diamidino-2-phenylindole. *Left,* types of tumors. **B,** FACS analysis of tumor infiltration 7 and 14 d after tumor inoculation. Percentage of tumor-infiltrating cells was calculated from the total number of the counted cells (1×10^5) and cells counted positive for the expression of the specific markers. *Columns,* mean of five independent counts; *bars,* SD. *Black columns,* B16F0-infiltrating cells; *white columns,* B16F0-UB-CCL21 – infiltrating cells. **C,** cytotoxicity of splenocytes (E:T ratio of 1:50) isolated from tumor-rejecting (*TR*), B16F0-inoculated (B16F0), and naive mice against various target cells (indicated in the panel) as determined by Annexin-based cytotoxicity assay. *Columns,* mean of five independent experiments; *bars,* SD. **D,** cytotoxicity of splenocytes (■ and ●) and $CD8^+$ T cells (□ and ○) isolated from tumor-rejecting mice against B16F0 (■ and □) and YAC-1 (● and ○) target cells at different E:T ratios. *Points,* mean of three independent experiments; *bars,* SD.

WT tumors started to develop (Fig. 5B), they completely cleared in all challenged mice within the first 10 days (Fig. 5C). Three of five mice that rejected secondary melanomas were challenged with a third i.d. inoculation of WT tumors 30 days after complete remission of the secondary tumors. Similarly, these tertiary tumors were completely rejected within 5 to 7 days after the third challenging inoculation. To date (20 months, more than two thirds of an average mouse life span), one of three mice remains alive and melanoma-free (the other two mice were euthanized to obtain splenocytes for the adoptive transfer experiments).

To investigate whether acquired protective immunity could be transferred to naive mice via splenocytes, C57BL6 naive mice ($n = 20$) were inoculated with primary WT melanoma as described above. Seven days later, these mice received 4×10^6 splenocytes collected either from animals that rejected secondary tumors or from control (B16F0 inoculated) mice. During first 4 days, tumors developed similarly in control and experimental animals (Fig. 5D). At later time points (7 days and thereafter), no delays in tumor outgrowth were observed in control mice, whereas melanomas rapidly regressed in all experimental animals. By day 15 (day 22 after tumor inoculation), WT tumors were diminished and seen on mouse skin as small pigmented spots with no palpable depth. Meanwhile, adoptive transfer of 1×10^5 $CD8^+CD62L^{high}CD44^{high}$ T_{CM} cells into tumor-bearing mice resulted in an even more rapid recognition of melanoma as deduced from the greater inhibition of tumor development (Fig. 5D). The outgrowth of melanomas in experimental animals was slowed within 3 days after adoptive transfer. During the next 7 days, tumors in all these mice regressed significantly and, by day 22, were seen on mouse skin as small pigmented spots. Taken together, these results clearly indicate that the observed rejection of primary CCL21-positive tumors resulted in acquisition of melanoma-specific protective immunity.

To test whether tumor-derived CCL21 can trigger immune responses sufficient for the rejection of distal melanomas, naive C57BL6 mice ($n = 10$) were inoculated with WT tumors and then, 5 days later, with B16F0-UB-CCL21 or B16F0-UB-Mock cells into the opposing flanks. Tumor development was monitored twice weekly for 4 weeks. B16F0 and B16F0-UB-Mock melanomas inoculated into the same animals developed at a similar rate (Fig. 5E,

solid and *open squares*). Meanwhile, inoculation of CCL21-expressing tumors resulted in the inhibition of B16F0 melanoma progression within the first 8 days. By day 27, WT tumors seemingly regressed and were slightly bigger than the B16F0-UB-CCL21 tumors (Fig. 5E, *solid* and *open circles*). Indirect immunofluorescent analysis of the excised B16F0 and B16F0-UB-CCL21 tumors showed their heavy infiltration with $CD8^+$ T cells (Fig. 3A), indicating involvement of cellular immunity in the inhibition of distant tumors. These data clearly indicate that immune responses activated against CCL21-positive melanoma are systemic and can target WT tumors.

Discussion

Previously, it has been shown that intratumoral injection of recombinant CCL21 or stable expression of the chemokine by tumor or dendritic cells significantly delayed tumor progression and stimulated cytotoxic immune responses (3–6). However, these previous attempts to elicit tumor-specific immunity using CCL21 *in vivo* resulted in partial tumor remission or complete regression of some but not all treated tumors. Here, we described an experimental system in which melanoma-derived CCL21 alone promoted activation of melanoma-specific systemic immune responses sufficient for rejection of the experimental melanoma *in vivo*. These striking results can be attributed to several differences in experimental protocol. First, we used the ubiquitin promoter to drive the expression of CCL21. This is a strong constitutive promoter that provided higher level of CCL21 expression and secretion when compared with the commonly used CMV promoter. Melanoma-derived CCL21 had no effect on melanoma cell proliferation and migration *in vitro* (data not shown) and on tumorigenic potential of the tumor *in vivo*. For example, CCL21-positive melanomas in immunodeficient B6.CB17-$Prkdc^{scid}$/SzJ mice developed with a similar rate as WT tumors in C57BL6 mice (Fig. 2B). Yet, a slight delay in progression of CCL21-positive tumors in SCID mice points to a possible contribution of $CCR7^+$ natural killer cells (12) to the melanoma targeting. Regardless of the contribution of the natural killer cells in restricting tumor growth, the robust expansion of all melanomas in SCID mice pointed to a crucial role of adaptive immunity in CCL21-dependent tumor regression.

The involvement of T lymphocytes in CCL21-mediated tumor targeting has previously been shown (4, 5). However, in contrast to previous findings, when B16F0-UB-CCL21 cells were used for tumor inoculation, melanomas were heavily infiltrated with $CD4^+CD25^-$ T cells,

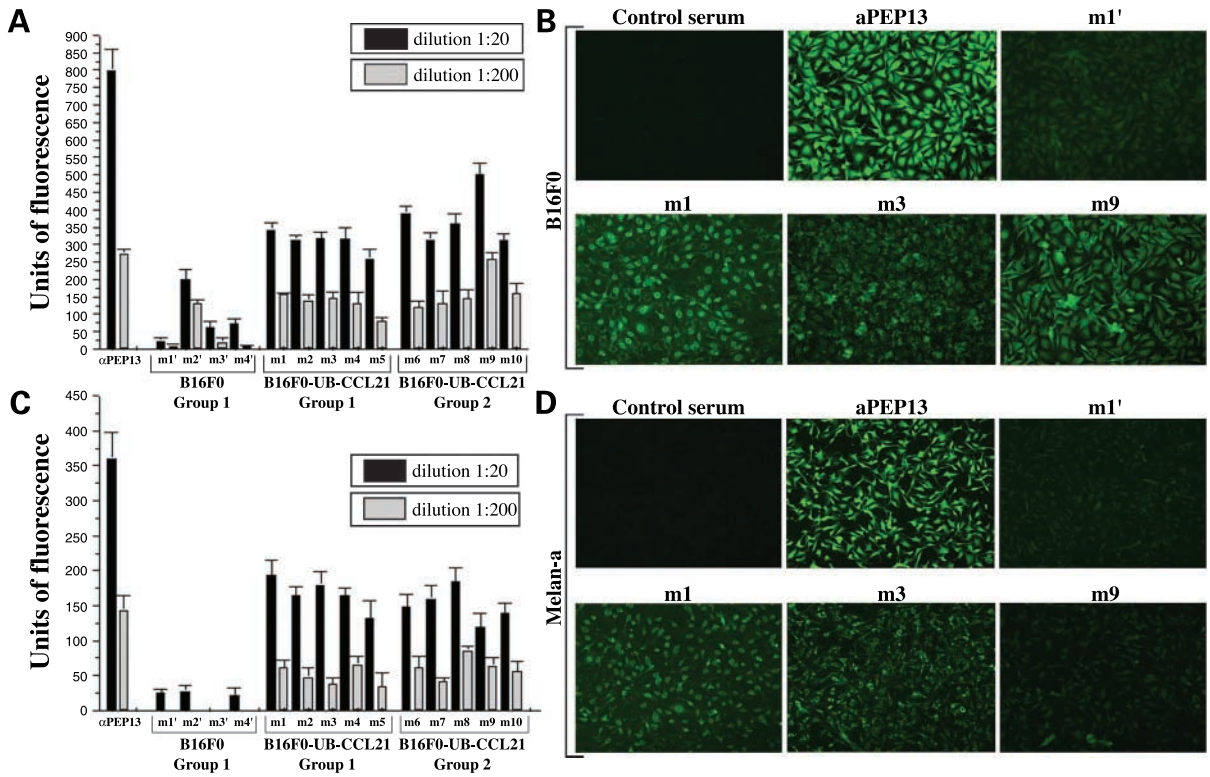

Figure 4. Analysis of melanoma-specific antibody production. **A,** relative reactivity of the sera against B16F0 cells. Sera were collected from mice inoculated with WT (*m1′–m4′*) or B16F0-UB-CCL21 melanomas (*m1–m10*). **B,** photographs of representative immunostainings of B16F0 melanoma cells with serum-derived antibodies. *Top,* source of sera or antibody. **C,** relative reactivity of the sera against Melan-a mouse melanocytes. Sera were collected from mice inoculated with WT or B16F0-UB-CCL21 melanomas. **D,** photographs of representative immunostainings of Melan-a cells with serum-derived antibodies. *Top,* source of sera or antibody. Data were collected from three independent measurements and presented as mean ± SD.

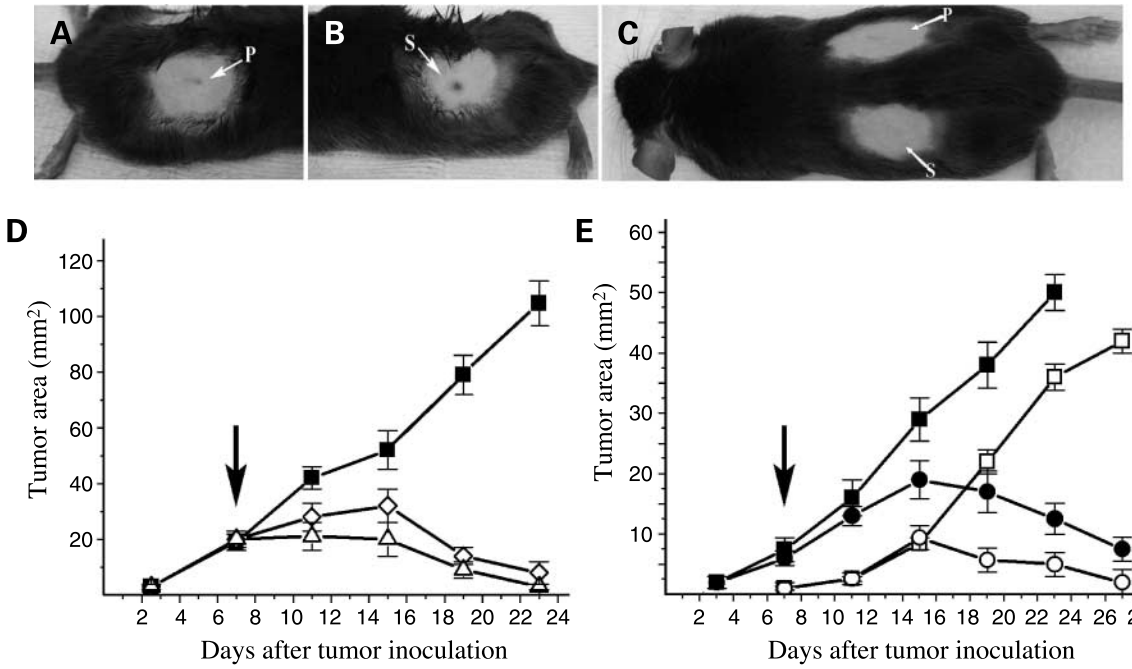

Figure 5. Challenge, adoptive transfer, and rejection of distant melanoma. **A,** photograph of mouse skin 40 d after inoculation of primary B16F0-UB-CCL21 melanoma. **B,** photograph of mouse skin 3 d after inoculation of the secondary B16F0 melanoma. **C,** photograph of primary (*P*) and secondary (*S*) melanoma sites 10 d after challenging inoculation. **D,** WT B16F0 melanoma outgrowth in naive mice that received control splenocytes (■) or splenocytes (◇) and T_{CM} cells (Δ) from tumor-rejecting mice. *Points,* mean; *bars,* SD. *Arrow,* points to the time of adoptive transfer. **E,** development of preestablished WT B16F0 melanomas (■ and ●) after inoculation of B16F-UB-Mock (□) and B16F0-UB-CCL21 (○) tumors at distant sites. *Arrow,* points to a time of B16F-UB-Mock and B16F0-UB-CCL21 tumor inoculation. Same shapes (■ and □ or ● and ○) represent the development of B16F0 and B16F-UB-Mock or B16F0-UB-CCL21 in the same animals. *Points,* mean; *bars,* SD.

which were detected in tumors as early as 48 h after inoculation (data not shown). These cells persisted in the tumor mass, and by 2 weeks, they represented 50% of all tumor-infiltrating $CD45^+$ leukocytes or 18% of all cells in the tumor. Taken together, these results suggest that elevated levels of melanoma-derived CCL21 promote infiltration of the tumors primarily with $CD4^+CD25^-$ T cells. Considering the results of recent investigation showing the ability of CCL21 to promote expansion and Th1 polarization of the T cells *in vitro* (13), our data suggest that melanoma-derived CCL21 not only directs the migration of naive $CD4^+CD25^-$ T cells to developing melanomas but also stimulates expansion of the primed $CD4^+$ T cells.

Development of antitumor vaccines often aims at generation of strong antitumor T-cell reactivity (14). Although CTLs are crucial effector cells against cancer, the high frequency of HLA class I antigen down-regulation in malignancies may limit the effectiveness of vaccines aimed at stimulating CTL responses (15, 16). In addition, recent studies showed that even a massive influx of activated $CD8^+$ T cells in a patient with malignant melanoma was not sufficient for inhibition of tumor progression (16). Moreover, previous attempts to use CCL21 for the stimulation of tumor-specific immunity (3–8), although successful in eliciting tumor-specific cytolytic $CD8^+$ T-cell–dependent responses, were not sufficient for eradication of the tumors *in vivo* in 100% of treated animals. Taken together, these findings suggest that generation of tumor-reactive CTLs is often inadequate for effective tumor immunotargeting. With respect to $CD4^+$ T cells, it has been shown that $CD4^+CD25^-$ T-helper (T_h) cells facilitate $CD8^+$ T-cell activation, survival, and function (17). In the absence of $CD4^+CD25^-$ T_h cells, $CD8^+$ memory T cells exhibit impaired functionality and an inability to control secondary tumor challenge (18). By contrast, $CD4^+CD25^+$ regulatory T cells were shown to suppress $CD8^+$ memory T cells (17). Here, we presented compelling evidence that generation of $CD4^+CD25^-$ T_h cells is critical for the induction, and most likely the maintenance, of melanoma-specific immune responses sufficient for complete tumor rejection.

Furthermore, we noted that different subsets of T lymphocytes were differentially distributed in tumors. For instance, $CD4^+CD25^-$ T cells were evenly distributed throughout the tumor mass, whereas $CD8^+$ T cells primarily accumulated at the periphery of tumor nodules at least during first 2 weeks after tumor inoculation. Interestingly, $CD11c^+$ tumor-infiltrating APCs as well as $CD4^+CD25^+$ regulatory T cells were also primarily found at the periphery. Because mature dendritic cells may be able to activate $CD8^+$ T cells in the absence of the $CD4^+$ T cells (19), our finding suggested that T_h-cell–independent priming of CTLs as well as inhibition of the CTL activity

by the regulatory $CD4^+CD25^+$ T cells occur on the periphery of the tumor. However, the intratumoral priming of naive $CD4^+CD25^-$ T lymphocytes and CCL21-stimulated differentiation into T_h1 and possibly T_h2 cells led to T_h-cell–dependent activation of cytotoxic and humoral immune responses. The simultaneous presence of melanoma-specific CTLs and melanoma-reactive antibodies in tumor-rejecting mice supported this notion.

Rechallenge experiments in tumor-rejecting mice additionally proved the immunologic mechanism of CCL21-mediated tumor rejection and acquisition of protective immunologic memory against melanoma. It is known that $CD8^+$ memory T cells are heterogeneous with respect to phenotypic markers, effector function, and homing capabilities. $CD8^+$ memory T cells have been divided into two broad categories: T_{CM} cells and effector memory T cells (T_{EM}). T_{CM} cells are antigen-experienced cells that constitutively express two surface molecules, CD26L and CCR7. By contrast, T_{EM} are antigen-experienced T cells in which these markers are significantly down-regulated. It has been suggested that these two distinctive populations of memory T cells have different functions: T_{EM} cells function as sentinels for the immediate protection from the peripheral challenge, whereas T_{CM} cells provide protection from the systemic challenge and can generate a second wave of effector cells. T_{CM} cells can preferentially migrate to secondary lymphoid organs or toward a higher gradient of CCL21 due to the expression of CCR7 and CD62L. These cells were also shown to be superior mediators of host protection against viral and bacterial challenge compared with T_{EM} cells (20–22). It is also been shown recently that adoptively transferred tumor-reactive $CD8^+$ T_{CM} cells are superior mediators of therapeutic antitumor immunity to an established cancer compared with T_{EM} cells when given in combination with a systemically administered tumor antigen vaccine (23). T_{CM} cells also have greater proliferative capacity on antigen reencounter compared with T_{EM} cells. However, the superiority of the T_{CM} cells has not been uniformly observed in all models.

In our experimental system, acquisition of strong melanoma-protective immunologic memory was confirmed by the adoptive transfer experiments. A significant regression of the WT melanomas in naive mice treated with either total population of the splenocytes or $CD8^+$ T_{CM} cells from tumor-rejecting animals confirmed the presence of melanoma-specific T-cell memory. Comparison of the kinetics of tumor regression in mice that receive either splenocytes or T_{CM} cells indicates the importance of T_{CM} lymphocytes in providing continuous rejuvenation of melanoma-specific cytolytic $CD8^+$ T cells in tumor regression. Additionally, this comparison showed that the total population of splenocytes triggered a delayed but more pronounced melanoma regression than T_{CM} cells alone (detected as rapid regression of tumors from days 15 to 19), suggesting that $CD4^+$ T-cell–dependent and possibly B-cell–dependent memory is required for immune-mediated melanoma rejection. Moreover, the rejection of the preestablished WT B16F0 tumors in mice, which were inoculated/immunized with B16F0-UB-CCL21 cells, directly points to the systemic nature of the induced immune responses and to the specificity toward melanoma.

Overall, in the current study, we show that elevated levels of the melanoma-derived CCL21 alone greatly enhanced infiltration of the $CD4^+CD25^-$, $CD8^+$ T lymphocytes, and $CD11c^+$ APC into tumor masses, leading to generation of melanoma-specific CTLs and high-titer melanoma-reactive antibodies. Interestingly, administration of the recombinant CCL21 in significantly greater amounts (3, 4) did not yield in similar responses, suggesting that tumor-derived chemokine is more potent for the future development of the chemokine-based vaccines.

The observed immune responses were sufficient for the rejection of primary, secondary, and tertiary tumors and for generation of strong, melanoma-specific protective immunity, transferable into naive mice via splenocytes and, specifically, T_{CM} cells. With potential clinical application in mind, we will further investigate and evaluate whether transient melanoma-specific expression of the chemokine in established tumors in combination with DNA-based melanoma vaccines will result in activation of similar immune responses and whether the proposed approach can be considered for treatment of established cutaneous melanoma.

Acknowledgments

We thank Drs. U. Rodeck and T. Sato for their helpful comments and discussion.

References

1. Lens MB, Dawes M. Global perspectives of contemporary epidemiological trends of cutaneous malignant melanoma. Br J Dermatol 2004; 150:179–85.

2. Cyster JG. Leukocyte migration: scent of the T zone. Curr Biol 2000; 10:R30–3.

3. Kirk CJ, Hartigan-O'Connor D, Nickoloff BJ, et al. T cell-dependent antitumor immunity mediated by secondary lymphoid tissue chemokine: augmentation of dendritic cell-based immunotherapy. Cancer Res 2001; 61:2062–70.

4. Sharma S, Stolina M, Luo J, et al. Secondary lymphoid tissue chemokine mediates T cell-dependent antitumor responses *in vivo*. J Immunol 2000;164:4558–63.

5. Hisada M, Yoshimoto T, Kamiya S, et al. Synergistic antitumor effect by coexpression of chemokine CCL21/SLC and costimulatory molecule LIGHT. Cancer Gene Ther 2004;11:280–8.

6. Yang S, Hillinger S, Ried K, et al. Intratumoral administration of dendritic cells overexpressing CCL21 generates systemic antitumor responses and confers tumor immunity. Clin Cancer Res 2004;10: 2891–901.

7. Yamano T, Kaneda Y, Huang S, Hiramatsu SH, Hoon DSB. Enhancement of immunity by a DNA melanoma vaccine against TRP2 with CCL21 as an adjuvant. Mol Ther 2006;13:194–202.

8. Elzaouk L, Pavlovic J, Moelling K. Analysis of antitumor activity elicited by vaccination with combinations of interleukin-12 DNA with gp100 DNA or the chemokine CCL21 *in vivo*. Hum Gene Ther 2006;17: 859–70.

9. Sodja C, Brown DL, Walker PR, Chaly N. Splenic T lymphocytes die preferentially during heat-induced apoptosis: NuMA reorganization as a marker. J Cell Sci 1998;111:2305–13.

10. Fischer K, Andreesen R, Mackensen A. An improved flow cytometric assay for the determination of cytotoxic T lymphocyte activity. J Immunol Methods 2002;259:159–69.

11. Antibodies: a laboratory manual. In: Harlow E, editor. Cold Spring Harbor (NY): Cold Spring Harbor Laboratory Press; 1988. p. 119.

12. Mailliard RB, Alber SM, Shen H, et al. IL-18-induced $CD83^+CCR7^+$ NK helper cells. J Exp Med 2005;202:941 – 53.

13. Flanagan K, Moroziewicz D, Kwak H, Horig H, Kaufman HL. The lymphoid chemokine CCL21 costimulates naive T cell expansion and Th1 polarization of non-regulatory $CD4^+$ T cells. Cell Immunol 2004;231: 75 – 84.

14. Rosenberg SA. Progress in human tumor immunology and immunotherapy. Nature 2001;411:380 – 4.

15. Gattinoni L, Klebanoff CA, Palmer DC, et al. Acquisition of full effector function *in vitro* paradoxically impairs the *in vivo* antitumor efficacy of adoptively transferred $CD8^+$ T cells. J Clin Invest 2005;115: 1616 – 26.

16. Harlin H, Kuna TV, Peterson AC, Meng Y, Gajewski TF. Tumor progression despite massive influx of activated CD8(+) T cells in a patient with malignant melanoma ascites. Cancer Immunol Immunother 2006;55: 1185 – 97.

17. Antony PA, Piccirillo CA, Akpinarli A, et al. $CD8^+$ T cell immunity against a tumor/self-antigen is augmented by $CD4^+$ T helper cells and hindered by naturally occurring T regulatory cells. J Immunol 2005;174: 2591 – 601.

18. Shedlock DJ, Shen H. Requirement for CD4 T cell help in generating functional CD8 T cell memory. Science 2003;300:337 – 9.

19. Dhodapkar MV, Krasovsky J, Steinman RM, Bhardwaj N. Mature dendritic cells boost functionally superior CD8(+) T-cell in humans without foreign helper epitopes. J Clin Invest 2000;105:R9 – 14.

20. Wherry EJ, Teichgraber V, Becker TC, et al. Lineage relationship and protective immunity of memory CD8 T cell subsets. Nat Immunol 2003;4: 225 – 34.

21. Castiglioni P, Gerloni M, Zanetti M. Genetically programmed B lymphocytes are highly efficient in inducing anti-virus protective immunity mediated by central memory CD8 T cells. Vaccine 2004;23:699 – 708.

22. Vaccari M, Trindade CJ, Venzon D, Zanetti M, Franchini G. Vaccine-induced $CD8^+$ central memory T cells in protection from simian AIDS. J Immunol 2005;175:3502 – 7.

23. Klebanoff CA, Gattinoni L, Torabi-Parizi P, et al. Central memory self/tumor-reactive $CD8^+$ T cells confer superior antitumor immunity compared with effector memory T cells. Proc Natl Acad Sci U S A 2005;102: 9571 – 6.

Molecular Cancer Therapeutics

Characterization of the CCL21-mediated melanoma-specific immune responses and *in situ* melanoma eradication

Laura Novak, Olga Igoucheva, Stephanie Cho, et al.

Mol Cancer Ther 2007;6:1755-1764.